Electronic Supplementary Material (ESI) for Journal of Materials Chemistry B

Supporting Information

Bio-Inspired Protein-Gold Nanoconstruct with Core-Void-Shell Structure: Beyond a Chemodrug Carrier

Xiangyou Liu, Wei Wei, Shijiao Huang, Shrong-Shi Lin, Xin Zhang, Chuanmao Zhang, Yuguang Du, Guanghui Ma, Mei Li, Stephen Mann and Ding Ma*

Background information about apoferritin (AFt), AFt-Au and AFt-AuFU

AFt-Au was prepared by reducing $AuCl_4^-$ with $NaBH_4$ in the cavity of apoferritin. Gold nanoparticles formed outside the protein cage were separated from the intra-ferritin gold nanoparticles by a sequence of separation procedures including centrifugation, size exclusion and ion exchange chromatography. TEM images (Fig. 1A) showed that all the outside Au nanoparticles were completely removed, leaving only the AFt-Au nanoconstructs, which were imaged as black dots (Au nanoparticles) surrounded by bright coronae (apoferritin). The obtained AFt-Au nanoparticle dispersions were very stable with respect to sedimentation; no turbidity or aggregation was observed in the dispersions even after more than two years at 4 °C. The results demonstrated that apoferritin coating conferred excellent stability on the AFt-Au nanoconstructs.

As molecules such as glucose and maltose have been shown to penetrate the apoferritin cavity,[1] it is reasonable to assume that 5-FU would be able to pass through the channels on apoferritin shell and enter the void space of the AFt-Au nanoconstructs where the drug could subsequently bind onto the surface of Au core.

Apoferritin, instead of AFt-Au, was also subjected to the same procedures as the preparation of AFt-AuFU. However, the final obtained solution showed no detectable fluorine signal in the ^{19}F-NMR spectrum, and showed no cytotoxicity towards HepG2 cells (data not shown), which indicated that 5-FU could not be easily captured by apoferritin cavity without the assistance of Au nanoparticles. In spite that 5-FU could freely disperse into the apoferritin cavity, the entered 5-FU could also readily leak out of the cavity because there was no affinity strong enough to anchor the drug molecules, which paid emphasis on the importance of Au nanoparticles.

As for Au nanoparticles without the apoferritin coating, *e.g.* citrate-stabilized Au nanoparticles, it was found that the color of the solution changed from red to dark purple after 5-FU was added, and finally the Au nanoparticles in the solution aggregated into black precipitates (see Fig. S4). Therefore, these Au nanoparticles (*i.e.* citrate-stabilized Au nanoparticles) were not suitable to be used as the 5-FU carriers. On the contrary, it was observed that no color changes or precipitation occurred after adding 5-FU to AFt-Au solution. These results showed the importance of the apoferritin shell. Without the apoferritin shell, Au nanoparticles could not efficiently work as drug carriers.

In conclusion, both the inner Au nano-core and the apoferritin shell of AFt-Au have separate and indispensable roles in the novel drug delivery system:

The inner Au core could:

1. Provide a surface to bind plenty of 5-FU *via* the interaction with –NH group of the drug, which enables AFt-Au to serve as an efficient drug carrier.
2. Induce the accumulation of cancer cells in S phase of cell cycle, by which AFt-Au sensitizes the cancer cells to 5-FU and enhances the anticancer efficacy of 5-FU.

The outer apoferritin shell could:

1. Constrain the growth of Au nanoparticles in the 8 nm cavity, therefore 3 nm Au particles with narrow size distribution and uniform shape can be obtained.
2. Confer excellent stability on AFt-Au.
3. Mediate the cellular uptake of Au particles and 5-FU *via* RME.
4. Impart cancer-cell selectivity to the drug.

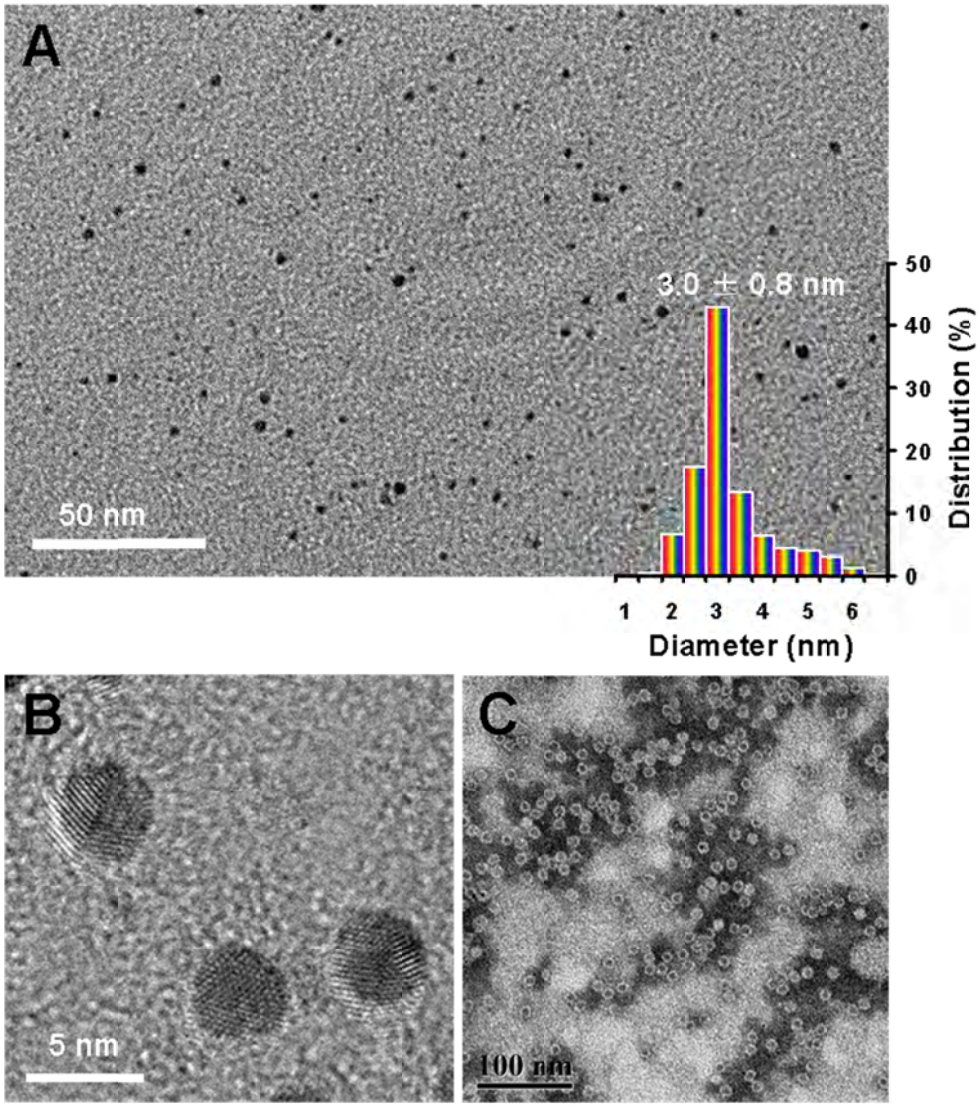

Fig. S1 (A) TEM image of AFt-Au without negative staining showing the existence of dispersed Au nanoparticles. The inset shows the corresponding size distribution of the Au nanoparticles (mean size = 3.0 nm). (B) HRTEM image of AFt-Au nanoconstructs showing lattice fringes of the gold nanoparticle core. (C) TEM image of negatively stained AFt-AuFU nanoconstructs.

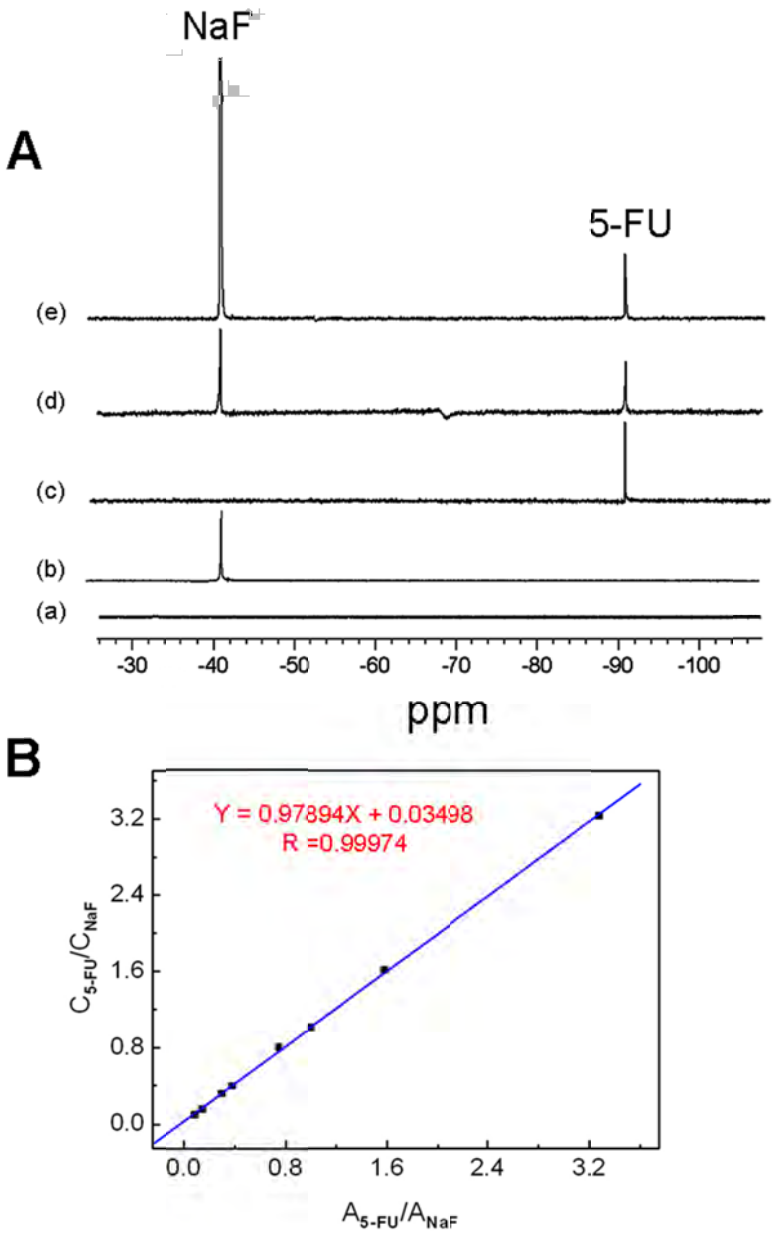

Fig. S2 (A) ^{19}F NMR spectra of (a) AFt-Au only, (b) NaF only, (c) 5-FU only, (d) AFt-AuFU nanoconstructs after removal of extrinsic 5-FU, and (e) simple mixture of AFt-Au, NaF and 5-FU. (B) Calibration curve used to quantify the amount of 5-FU in AFt-AuFU.

The ^{19}F NMR spectra were performed on Varian-300 MercuryPlus Spectrometer. Regular 5 mm NMR tubes were used and the detections were carried out at room temperature. CF_3CO_2D was applied as external standard and referred to 0 ppm. NaF was used as internal standard for

quantitative analysis. The scanning time (number of transmit), from minutes to hours, was determined by the results of spectra till unambiguous plot and integration were obtained.

In Fig. S2A, the spectrum (e) illustrated that the addition of NaF to 5-FU gave signals of NaF and 5-FU only and no other signal was detected. The chemical shifts of NaF and 5-FU were determined by known compounds as shown in spectrum (b) and (c). It was concluded, by comparing the spectra of (b), (c) and (e), that NaF would not influence the experimental results and could be used as internal standard. Without involvement of F atom, no signal was detected for the solution of AFt-Au (spectrum (a)). The spectrum of the prepared AFt-AuFU was shown in spectrum (d), wherein signal corresponding to 5-FU was detected (-91 ppm); the signal at lower field (-41 ppm) was NaF which was added as internal standard for quantitative analysis.

The calibration curve in Fig. S2B was obtained by plotting the concentration ratio of 5-FU/NaF ($C_{5\text{-}FU}/C_{NaF}$) *versus* the integration ratio of 5-Fu/NaF ($A_{5\text{-}FU}/A_{NaF}$). Linear relationship was obtained. By applying the calibration curve, the 5-FU concentration of the prepared AFt-AuFU could be calculated from the known integration ratio ($A_{5\text{-}FU}/A_{NaF}$) and known concentration of NaF added to the experimental system.

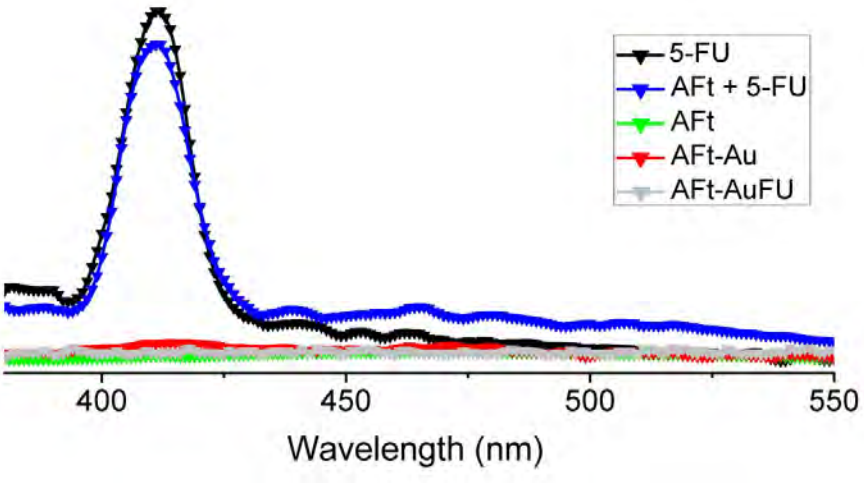

Fig. S3 Emission spectra (λ_{EX} = 360 nm) of 5-FU, AFt, AFt-Au, AFt-AuFU and a mixture of AFt and 5-FU (AFt + 5-FU). The drug concentrations in 5-FU, AFt-AuFU and AFt + 5-FU were equal, while samples AFt + 5-FU, AFt, AFt-Au and AFt-AuFU had the same protein concentrations. The conjugation of 5-FU with the intra-apoferritin Au particles was demonstrated by the quenching of the drug's fluorescence in the emission spectrum of AFt-AuFU.

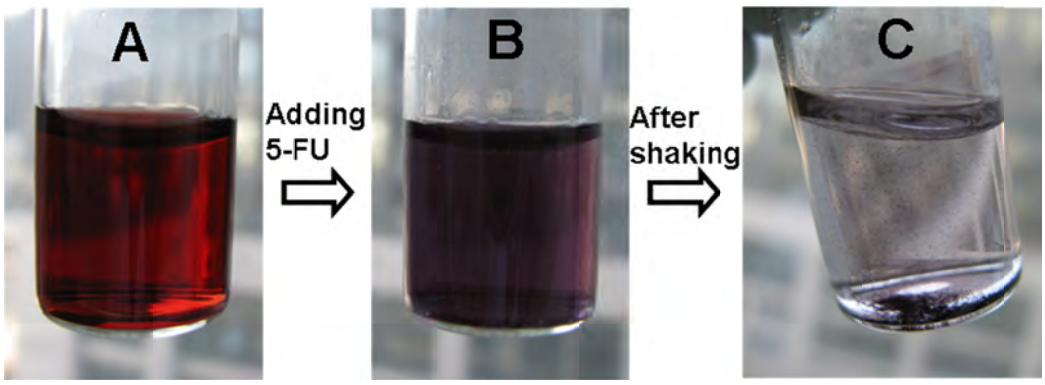

Fig. S4 (A) Aqueous solution of citrate-stabilized Au nanoparticles in 0.1 M citrate buffer (pH 6.0). (B) The solution in (A) after 5-FU was added for several minutes showing color change due to particle aggregation. (C) The solution in (B) after it was shaken (200 rpm) at 35 °C for ~ 0.5 h showing precipitate.

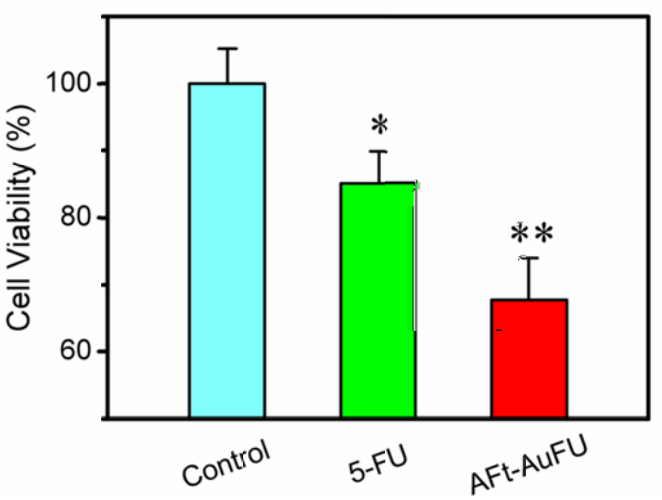

Fig. S5 Cytotoxicity of free 5-FU and AFt-AuFU under the condition wherein the intracellular 5-FU concentrations were equal. HepG2 cells were pre-treated with 5-FU (240 μM) or AFt-AuFU (120 μM) for 6 h, after which the cell viability remained 100% and the internalized 5-FU amounts were identical. Then the cells were rinsed twice to remove all extracellular 5-FU or AFt-AuFU, a fresh culture medium was added, and the cells were cultured for 48 h. Finally, CCK-8 solution was added to assay the cell viability. HepG2 cells without any treatment were used as control. *$P < 0.05$, **$P < 0.01$, *versus* the control.

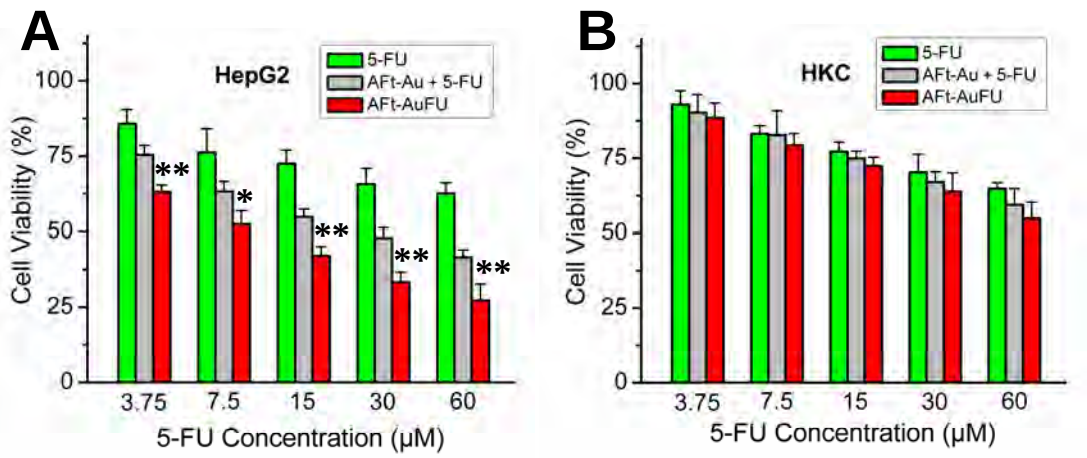

Fig. S6 Comparison of the cytotoxicity of free 5-FU, AFt-Au + 5-FU, and AFt-AuFU in HepG2 (A) and HKC (B) cells. The AFt-Au + 5-FU sample was prepared by the immediate mixture of AFt-Au and 5-FU just before use. This mixture was not subjected to shaking for 30 h or centrifugal filtration. *$P < 0.05$, **$P < 0.01$, *versus* corresponding AFt-Au + 5-FU groups.

Although AFt-Au had no obvious influence on the viability of HepG2 and HKC cells (see Fig. 2A and Fig. 4A), AFt-Au + 5-FU showed a higher cytotoxicity than free 5-FU, but did not outperform AFt-AuFU in Fig. S6. In the AFt-Au + 5-FU mixture, 5-FU could not be concomitantly transported into cells with AFt-Au as it was not loaded within AFt-Au. Therefore, the internalized 5-FU concentration could not increase by AFt-Au, which in turn would compromise the final cytotoxicity of AFt-Au + 5-FU mixture. Even if the internalized AFt-Au nanoconstructs induced the accumulation of cancer cells in S phase of cell cycle, this might not occur synergistically with 5-FU activity as the two components (*i.e.* AFt-Au and 5-FU) are separated, not conjugated. Therefore, AFt-Au in the AFt-Au + 5-FU mixture did not efficiently potentiate the cytotoxicity of 5-FU. Consequently, the AFt-Au + 5-FU mixture was not as cytotoxic as the AFt-AuFU nanoconstruct.

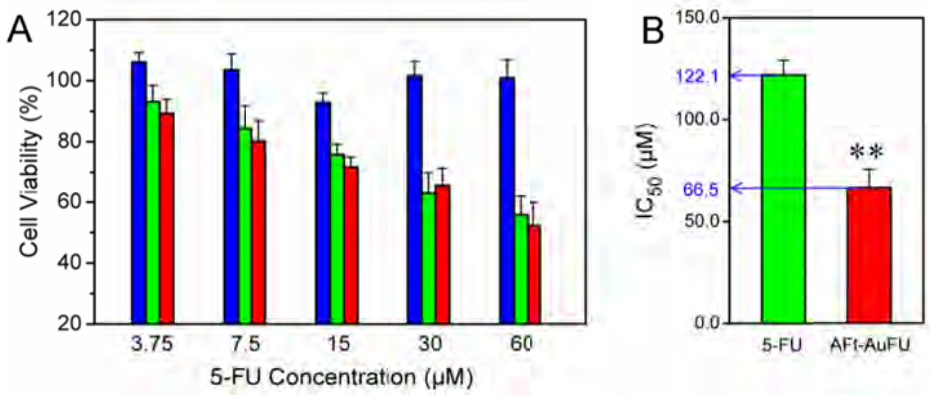

Fig. S7 Cytotoxicity of AFt-AuFU nanoconstruct to L02 cells. (A) Viability of L02 cells after treatment with AFt-Au (blue), 5-FU (green) or AFt-AuFU (red) for 48 h. In each group, the Au concentrations of AFt-Au and AFt-AuFU are identical. (B) IC_{50} values of free 5-FU and AFt-AuFU in L02 cells. $^{**}P < 0.01$, *versus* corresponding 5-FU group.

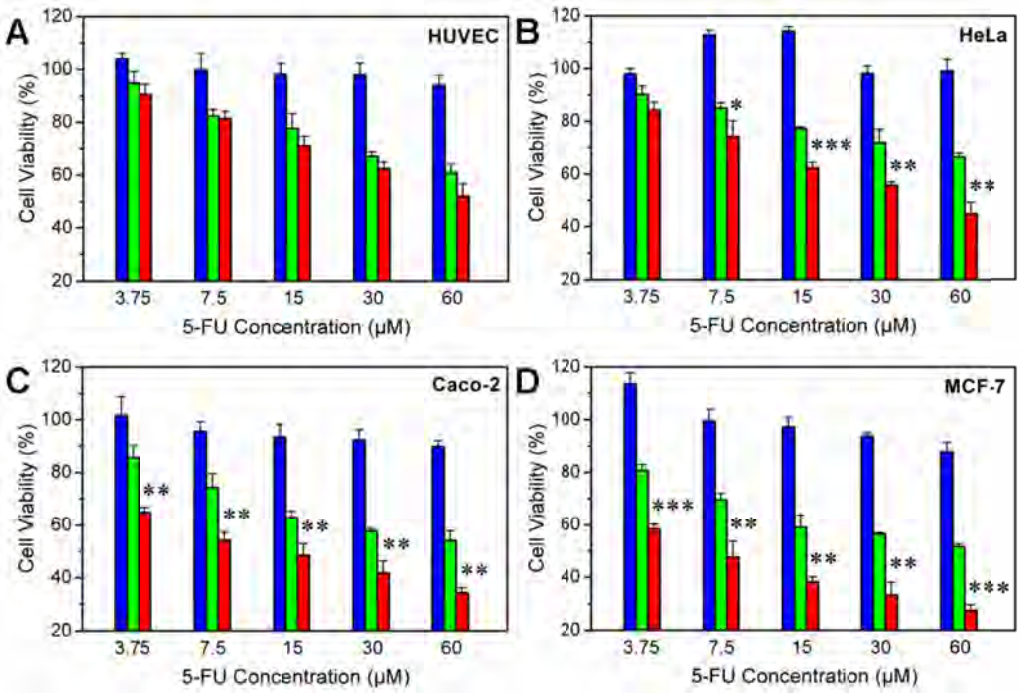

Fig. S8 Cell viability of HUVEC (A), HeLa (B), Caco-2 (C) and MCF-7 (D) cells after treatment with AFt-Au (blue), free 5-FU (green) and AFt-AuFU (red) for 48 h. In each group, the Au concentrations of AFt-Au and AFt-AuFU are identical. *$P < 0.05$, **$P < 0.01$, ***$P < 0.001$, *versus* corresponding 5-FU groups.

Electronic Supplementary Material (ESI) for Journal of Materials Chemistry B

Table S1 Summary of IC_{50} values of 5-FU and AFt-AuFU in different types of cells.

Cell type	IC_{50} (μM)	
	5-FU	AFt-AuFU
HKC	126.5	85.1
L02	122.1	66.5
HUVEC	116.3	65.4
HepG2	138.3	9.2
HeLa	228.5	45.9
Caco-2	78.1	12.1
MCF-7	70.0	6.7

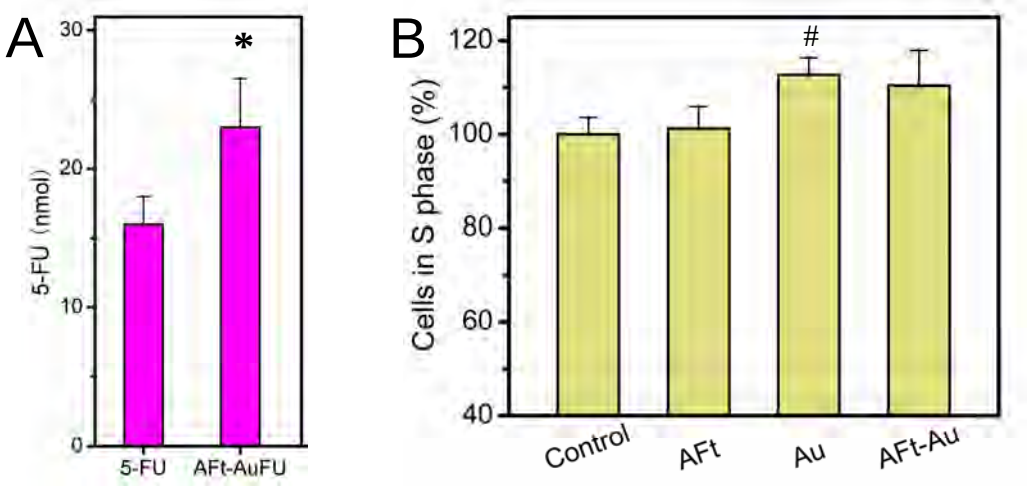

Fig. S9 (A) Internalized amount of 5-FU in HKC cells after treatment with free 5-FU (120 μM) or AFt-AuFU (120 μM) for 6 h. (B) Flow cytometric analysis of HKC cells in S phase. HKC cells were treated with AFt, Au, AFt-Au or left untreated (control). The results were expressed as a percentage of the amount of S-phase cells in the control (100%). *$P < 0.05$, *versus* corresponding 5-FU group. #$P < 0.05$, *versus* the control.

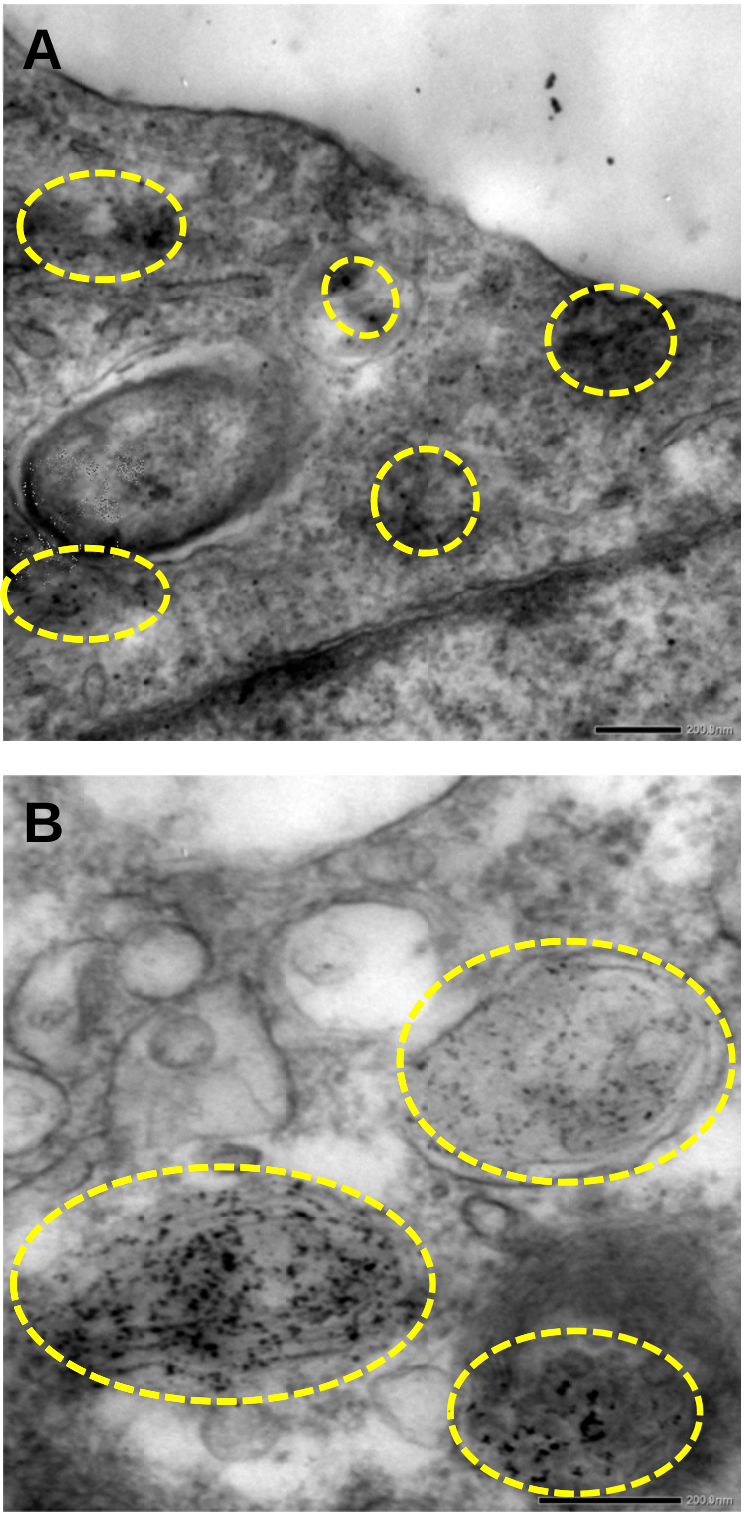

Fig. S10 Representative TEM images of HKC (A) and HepG2 cells (B) with internalized AFt-Au nanoparticles which were shown in yellow dash-line circled areas. It was observed from the TEM images that more AFt-Au nanoparticles were internalized in HepG2 than in HKC cells. Scale bars: 200 nm.

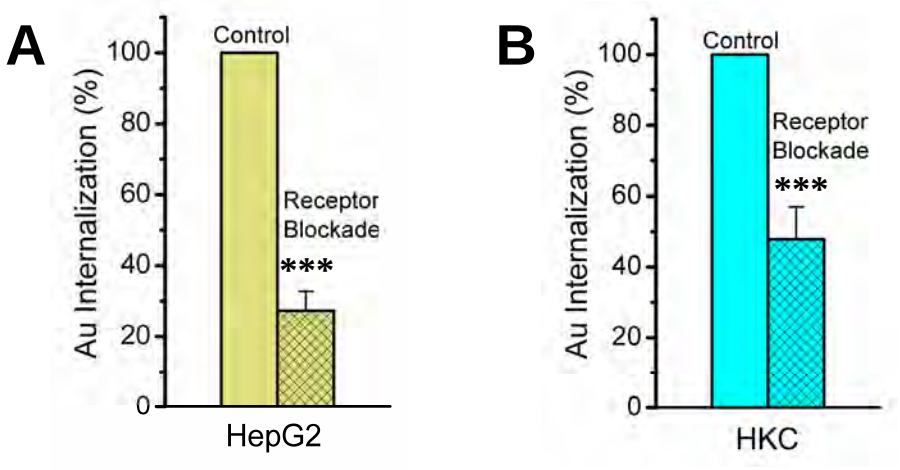

Fig. S11 The internalization of AFt-Au in HepG2 (A) and HKC (B) cells before (control) and after the AFt receptors were blocked. The results were expressed as percentage of the internalized AFt-Au level in the control in terms of Au amount. Blocking the AFt receptors in the two types of cell lines resulted in a more than 50% decrease of internalized AFt-Au, suggesting that RME played an important role in the cellular uptake of AFt-Au. ***$P < 0.001$, *versus* the control.

References

1. D. W. Yang and K. Nagayama, *Biochem. J.*, 1995, **307**, 253-256.